JOURNAL OF MATERIALS SCIENCE 30 (1995) 5833–5840

Environmental stress cracking of PVC and PVC–CPE

Part III *Crack growth*

J. BREEN
TNO Plastics and Rubber Research Institute, P.O. Box 6031, 2600 JA Delft, The Netherlands

The fracture toughness of polyvinylchloride (PVC) and PVC modified with 10% chlorinated polyethylene (PVC–CPE) was studied in vapour and in liquid environments by crack growth measurements on single-edge notch specimens under three-point bending at 23 °C. In addition, some results obtained in air at lower temperatures are presented. The fracture toughness is quantified by a stress intensity factor leading to failure after a given loading period. It is shown that for a given slow crack growth rate at 23 °C, the environment hardly affects the fracture toughness of PVC. In contrast, the slow crack growth in PVC–CPE at 23 °C is accelerated by the presence of benzene vapour, *n*-octane/benzene mixtures and gas condensate. A decrease in temperature results in an increase in fracture toughness, both for PVC and for PVC–CPE. A Dugdale model to describe the craze ahead of the crack was used to analyse the observed changes in fracture toughness.

1. Introduction

Environmental stress cracking of polyvinylchloride (PVC) and PVC modified with 10% chlorinated polyethylene (PVC–CPE) materials in natural gas environments has been studied in order to obtain insight into the durability and safety of the PVC and PVC–CPE gaspipes used in the low-pressure part of the natural gas distribution network in the Netherlands.

The environmental stress cracking capacity of natural gas components on PVC and PVC–CPE gaspipe materials has been quantified by craze initiation, craze growth and by crack propagation measurements. A previous investigation has shown that the decrease of the initiation stress for surface crazes in enriched natural gas environments and in natural gas condensate can be explained by local plasticization, which occurs due to a rapid sorption of gas components in the vicinity of defects acting as stress raisers [1]. The plasticization leads to a decrease of the local drawing stress, which is proportional to the craze initiation stress.

The logarithmic growth of surface crazes can also be interpreted in terms of a local drawing process [2]. The decrease of the stress with increasing distance from the stress raiser results in a decrease of the growth rate of surface crazes.

The unnotched PVC and PVC–CPE test strips failed in either a ductile or a brittle way, depending on the enriched natural gas environment used [2]. A brittle failure occurs after a continuous or a renewed craze growth process. When the craze growth ceases after some period and no renewed craze growth occurs, a ductile failure is observed.

In order to evaluate the brittle failure in PVC and PVC–CPE more thoroughly, the crack propagation of notched test strips was studied in enriched natural gas environments. The experimental apparatus for these measurements resembles closely that of the slow crack growth experiments on PE (polyethylene) pipe materials (see, for example, [3–5]).

Crack propagation studies on PVC (pipe) materials have been reported less frequently [6–8]. Instead of actual crack growth measurements, critical stress intensity criteria for crack growth have been quantified by various authors [7, 9–11]. The critical stress intensity factor is not a unique quantity. For example, different values of the critical stress intensity factor for crack initiation, for rapid crack growth and for slow crack growth, have been defined [9].

The time-dependence of the crack growth is related to a drawing process in front of the crack tip [12–15]. This plastic zone is associated with a craze. The crack growth is related to the craze growth and the stability of the craze fibrils. The shape of the craze in front of the crack tip is determined by the stress distribution at the craze interface and the load carried by the craze fibrils [15]. Both the stress at the craze interface and the load carried by the craze fibrils can be reduced in gas or liquid environments due to plasticization. The shape of the craze observed in gas environments therefore differs from that observed in air [16]. Notwithstanding the influence of gas and liquid environments on the stability of the craze fibrils and on the craze growth, the fracture toughness does not seem to be affected very much by plasticization [16].

This article describes the influence of gas components on the crack growth of notched PVC and

0022–2461

PVC–CPE gaspipe materials. It will be shown that the fracture toughness for PVC and PVC–CPE is affected by the plasticization in a different manner. The variations observed in the fracture toughness are explained in terms of variations in the drawing stress, the modulus, the crack tip opening displacement and the craze–fibril stability.

2. Theory

2.1. Craze dimensions

When a notched specimen is loaded, a craze will grow ahead of the crack. The Dugdale model can be used to predict the size of this craze [13, 14]. The plastically deformed zone formulated in the Dugdale model is associated with the craze. In Fig. 1, the Dugdale zone is presented schematically.

The length of the Dugdale zone is, in a first approximation, given by [13]

$$a_c = \frac{\pi}{8}\left(\frac{K_I}{\sigma_c}\right)^2 \quad (1)$$

where K_I represents the applied stress intensity factor, and σ_c the constant stress over the Dugdale zone.

Equation 1 does not hold exactly for the craze length of PVC materials [14]. The stress intensity factor calculated from the craze dimension is about a factor 3 lower than the measured one. The explanation for the difference is thought to be the presence of a non-voided yielded zone which coexists with the craze zone.

Instead of the craze length, the crack tip opening displacement can be measured. The crack tip opening displacement equals the length of the craze fibrils at the craze–crack transition. From the relation between the stress intensity factor and the strain energy release rate, and the fact that the work done at the crack tip is proportional to the craze thickness and to the stress carried by the craze, a relation between the crack tip opening displacement and the craze length can be obtained. This equation is [13]

$$a_c \approx \frac{\pi}{8}\frac{E}{\sigma_c}\delta_c \quad (2)$$

where δ_c represents the crack tip opening displacement and E the Young's modulus. a_c and σ_c are,

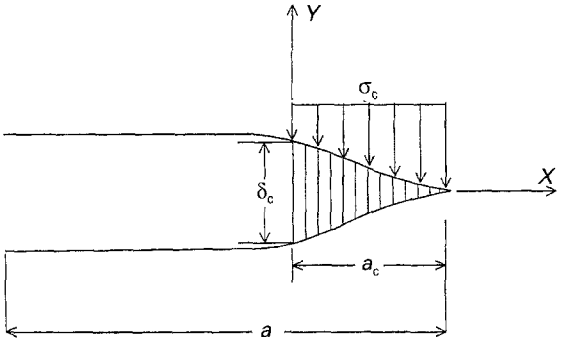

Figure 1 Illustration of the Dugdale plastic zone, where a constant stress, σ_c, applies. Definition of the quantities a (crack length), a_c (length of the Dugdale zone) and δ_c (crack tip opening displacement) is shown.

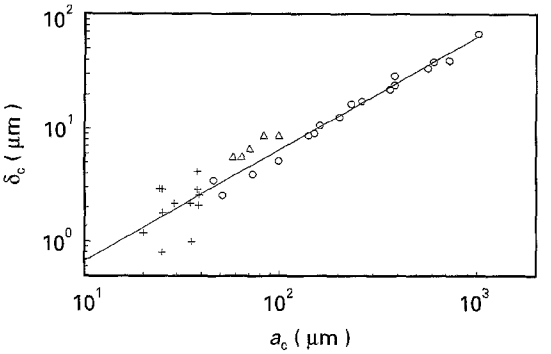

Figure 2 Crack tip opening displacement versus craze length. (+) PMMA [17], (△) PC [18], (○) PVC [19].

respectively, the craze length and the stress carried by the craze. The relation between crack tip opening displacement and craze length shown in Fig. 2 is given by

$$a_c = 15\,\delta_c \quad (3)$$

From these data and Equation 2, a realistic value for the ratio $E/\sigma_c \approx 40$ is calculated.

2.2. Craze growth criteria

A craze growth criterion for a craze ahead of a crack tip differs from that for a surface craze [2]. Whereas the craze growth of a surface craze is determined by the decreasing stress level away from the craze initiation point, the stress level experienced by a craze ahead of a growing crack will be constant or will increase with the crack length.

Growth criteria for a crack tip craze are usually given in terms of a critical stress intensity factor or a critical strain energy release rate [9, 13]. A simple equation for the critical stress intensity factor can be derived from the Equations 1 and 2. This equation is [13]

$$K_c \approx (\delta_c\,\sigma_c\,E)^{1/2} \quad (4)$$

where K_c represents the critical stress intensity factor.

2.3. Time-dependence

The viscoelastic behaviour shown by polymeric materials under a constant stress results in a time-dependent process which is known as creep. The viscoelastic behaviour is characterized by a decreasing modulus with increasing loading time. Furthermore, the drawing stress decreases with increasing loading time.

The critical stress intensity factor defined in Equation 4 for craze growth is a function of both the modulus and the drawing stress [13]. Therefore, the critical stress intensity factor will decrease when the time to failure increases. An increase in time to failure corresponds with a decreasing crack growth rate. The influence of both the environment and the temperature on time-dependent properties can be incorporated in the drawing stress and the modulus.

3. Experimental procedure

The PVC and PVC–CPE gaspipe materials used in this study were 2.7 mm thick. Specimens, in which the

plane-strain condition holds during the crack growth, are hard to realize. Circumferential rings taken from the pipe, cut into two equal arch segments and notched afterwards, can fulfil this condition for the thick-walled pipes [10]. For thin-walled pipes, this procedure is not valid.

Therefore, a different specimen was used (see Fig. 3). This specimen consisted of a rectangular 2.7 mm thick PVC or PVC–CPE test strip which was constrained by two epoxy layers [20]. Rectangular test strips were obtained from the PVC and PVC–CPE pipes by compression moulding at 125 °C of the curved strips cut longitudinally from the pipes. Epoxy layers were adhered to these PVC and PVC–CPE test strips. After the V-shaped notch was machined into the specimen, a sharp notch was introduced by a razor blade and the specimen was annealed for 3 h at 95 °C.

The stress intensity factor for a single-edge notch specimen under three-point bending is given by [20]

$$K_I = \frac{3}{2}\frac{PL}{tW^2} Y a^{1/2} \quad (5)$$

where P is the load, L the loading length, t the thickness, W the width, Y the geometrical factor, and a the notch depth.

The geometrical factor, Y (see Equation 5), was obtained experimentally from compliance versus crack length measurements and numerically by finite elements calculations [20].

In a number of experiments the bending was recorded. The frame with the outer loading points was combined with the rod to which the dead loads were attached. In order to study the influence of gas components and liquids, the three-point bending equipment was placed in a glass bell. A teflon bellow is used to prevent leakage between the bearing and the rod of the loading system.

In Fig. 4, the bending of a single-edge notch specimen is illustrated. The width, W, the loading length, L, the load, P, and the bending angle, θ, are defined for this type of specimen.

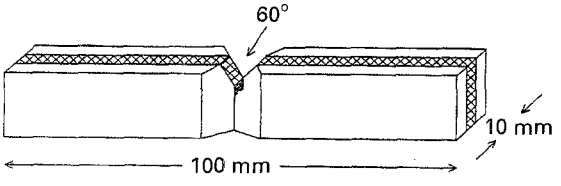

Figure 3 The single-edge notch specimen used. Epoxy layers are used to obtain crack growth under plane-strain conditions.

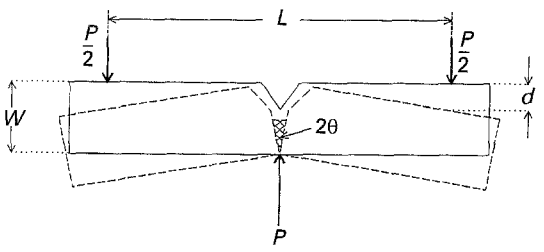

Figure 4 Illustration of three-point bending; definition of symbols.

4. Results

Crack growth experiments were performed in different environments (air, natural gas, benzene enriched natural gas, natural gas condensate and *n*-octane/benzene mixtures) at 23 °C to obtain the time to failure as a function of the applied stress. In some of the 23 °C measurements, the bending was recorded as a function of the loading time. The bending curves obtained in this way are presented. The fracture toughness was also studied at lower temperatures in air and some natural gas environments. The lowest temperature studied was − 25 °C. A summary of the temperature-dependent measurements in air is also given.

4.1. Fracture toughness versus environment

The time to failure versus the applied stress intensity is shown in Figs 5–8 for PVC–CPE and PVC in air, natural gas enriched with 60 000 p.p.m. benzene, *n*-octane, low-pressure condensate and high-pressure condensate. Low-pressure condensate represents the condensate found in the low-pressure (< 4 bar) part of the natural gas distribution system, and the high-pressure condensate represents the condensate found

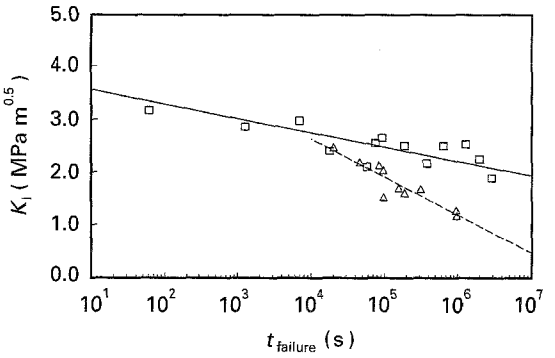

Figure 5 Stress intensity factor, K_I, as a function of the time to failure, t, for PVC–CPE at 23 °C in (□) air and (△) natural gas enriched with 60 000 p.p.m. benzene. (——) Least-squares fit of the data obtained in air; (— —) least-squares fit of the data obtained in 60 000 p.p.m. benzene.

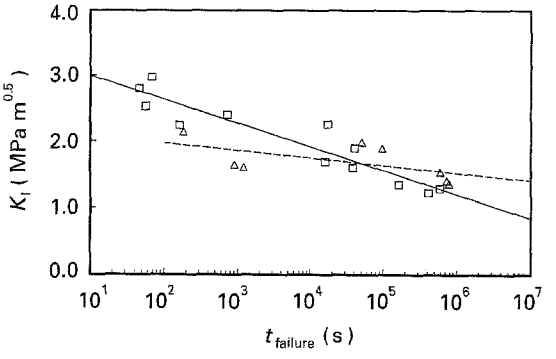

Figure 6 Stress intensity factor, K_I, as a function of the time to failure, t, for PVC at 23 °C in (□) air and (△) natural gas enriched with 60 000 p.p.m. benzene. (——) Least-squares fit of the data obtained in air; (— —) least-squares fit of the data obtained in 60 000 p.p.m. benzene.

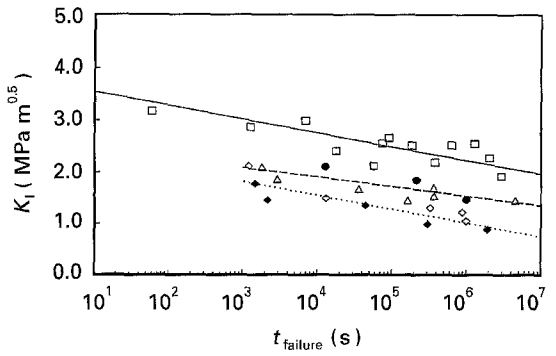

Figure 7 Stress intensity factor, K_I, as a function of the time to failure, t, for PVC–CPE at 23 °C in (□) air, (△) *n*-octane, (●) low-pressure condensate, (◆) high-pressure condensate, and (◇) (90%/10%) *n*-octane/benzene mixture. (——) Least-squares fit of the data obtained in air; (— —) least-squares fit of the data obtained in *n*-octane and low-pressure condensate; (···) least-squares fit of the data obtained in (90%/10%) *n*-octane/benzene and high-pressure condensate.

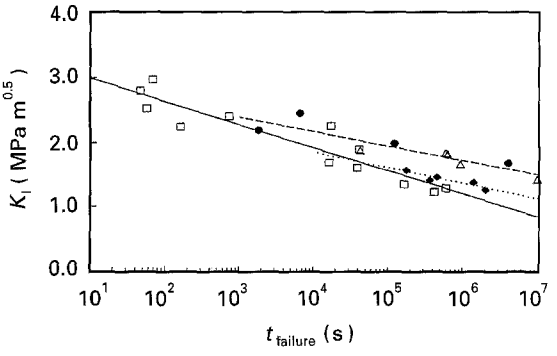

Figure 8 Stress intensity factor, K_I, as a function of the time to failure, t, for PVC at 23 °C in (□) air, (△) *n*-octane, (●) low-pressure condensate and (◆) high-pressure condensate. (——) Least-squares fit of the data obtained in air; (— —) least-squares fit of the data obtained in *n*-octane and low-pressure condensate; (···) least-squares fit of the data obtained in high-pressure condensate.

in the high-pressure (> 8 bar) part. High-pressure condensate contains hydrocarbon molecules with an average carbon number of 10 and amounts of benzene, toluene and xylene of about 10%. Low-pressure condensate contains hydrocarbon molecules with an average carbon number of 15, and no significant amounts of benzene, toluene and xylene.

The scatter in the data points is thought to be a result of differences in the ratio of crack length to specimen width and in the machining of the specimens. The crack length to specimen width ratio is 0.30 ± 0.05.

It was found that the failure curves (applied stress intensity factor versus time to failure) in air and natural gas coincide within the accuracy of the measurement. Therefore, the change in failure curve obtained in natural gas enriched with 60 000 p.p.m. benzene shown in Figs 5 and 6 is determined by the action of the benzene vapour. A concentration of 60 000 p.p.m. benzene at 23 °C means a relative saturation of about 50%.

It is noticed that the action of the benzene vapour is detrimental for PVC–CPE (see Fig. 5). Single-edge notch PVC–CPE specimens fail in 60 000 p.p.m. benzene at a considerably lower stress intensity factor than those in air. The crack growth in PVC–CPE is thus stimulated in the presence of benzene vapour. On the contrary, the crack growth of single-edge notch PVC specimens seems to be decelerated by the presence of 60 000 p.p.m. benzene (see Fig. 6).

When the results obtained on PVC are compared with those obtained on PVC–CPE, it is clear that crack growth in air will occur in notched PVC gaspipe material at lower stress levels than in notched PVC–CPE gaspipe material. It was found that the same argument holds for the crack growth of these materials in natural gas at 23 °C. However, the crack growth of notched gaspipe PVC material in natural gas with 60 000 p.p.m. benzene at a stress intensity below about 1.5 MPa m$^{1/2}$ is slower than that of the notched gaspipe PVC–CPE material under identical conditions.

An analogous situation is observed comparing the results of PVC–CPE and PVC shown in Figs 7 and 8, respectively. In Fig. 7, the sequence of decreasing stress intensity factor for a given time to failure is air > *n*-octane ≈ low-pressure condensate > high-pressure condensate ≈ 90%/10% *n*-octane/benzene. The decrease in stress intensity factor resulting in crack growth can thus be enhanced by increasing the benzene concentration in the mixture. Nevertheless, aliphatic compounds also affect the crack growth of notched PVC–CPE gaspipe material.

The sequence of decreasing stress intensity factor for a given time to failure for PVC (Fig. 8) is *n*-octane ≈ low-pressure condensate > high-pressure condensate ≈ air. In *n*-octane and low-pressure condensate, the stress intensity factor and thus the fracture toughness of notched PVC specimens is improved relative to the values found in air. The influence of the benzene concentration on the stress intensity factor corresponding to a given time to failure is less obvious for PVC. Low benzene concentrations seem to be beneficial, whereas high benzene concentrations seem to be detrimental.

4.2. Bending curves

In order to obtain more information on the different crack growth behaviours of PVC and PVC–CPE, the bending of the outer loading points was recorded (see Fig. 4). The bending, d, is related to the bending angle, θ. In a first approximation, the following relation holds

$$\theta = \frac{d}{40} \tag{6}$$

Some results on the bending experiments are shown in Figs 9–12. The start of the bending experiment is not well-defined, due to the hand-loading procedure. Therefore, the bending corresponding with $d = 0$ was estimated.

The bending curves can be divided in three regions:

1. an initial bending which is related to the initiation of a craze ahead of the crack;
2. a constant bending rate which is related to crack growth (the failure of the craze fibrils at the crack tip

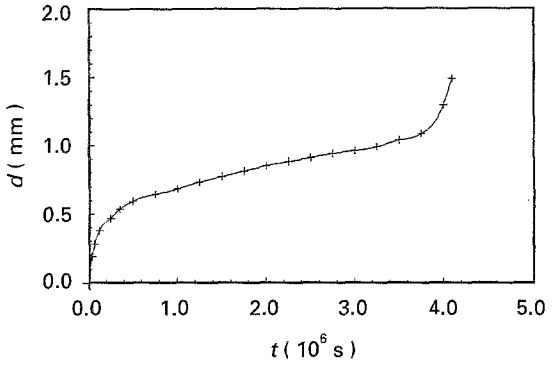

Figure 9 Bending, d, versus the loading time, t, for PVC–CPE in air. $K_I = 2.2\ MPa\,m^{1/2}$; $a/W = 0.35$; $t_{failure} = 4.1 \times 10^6$ s.

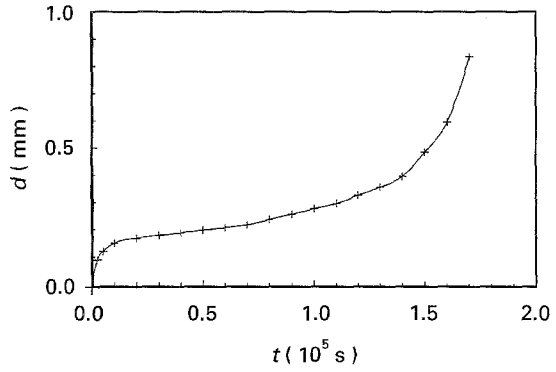

Figure 10 Bending, d, versus the loading time, t, for PVC in air. $K_I = 1.6\ MPa\,m^{1/2}$; $a/W = 0.33$; $t_{failure} = 1.7 \times 10^5$ s.

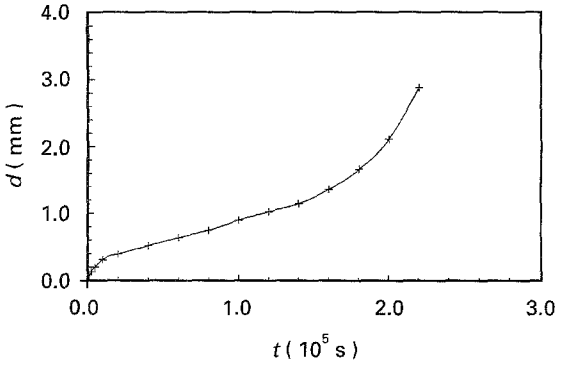

Figure 11 Bending, d, versus the loading time, t, for PVC–CPE in natural gas enriched with 60 000 p.p.m. benzene. $K_I = 1.7\ MPa\,m^{1/2}$; $a/W = 0.28$; $t_{failure} = 2.2 \times 10^5$ s.

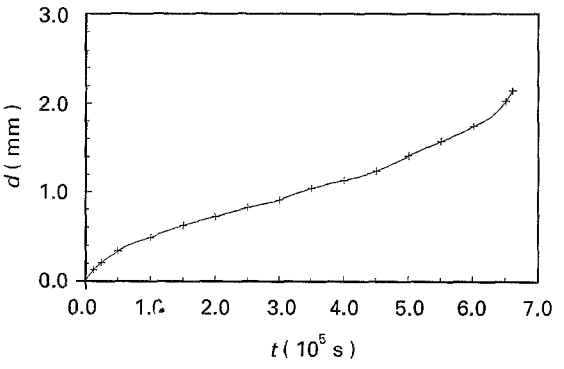

Figure 12 Bending, d, versus the loading time, t, for PVC in natural gas enriched with 60 000 p.p.m. benzene. $K_I = 1.9\ MPa\,m^{1/2}$; $a/W = 0.35$; $t_{failure} = 7.0 \times 10^5$ s.

and the creation of new craze fibrils at the head of the plastically deformed zone);

3. an increasing bending rate which is related to the acceleration of the crack growth process.

At the transition from region 1 to region 2, broken craze fibrils can be observed by a microscope (magnification $\times 100$) positioned above the notch. Analogous results were found by Lu and Brown for PE materials [3].

Notwithstanding some speculation about the exact starting point of the bending measurement, the bending angle at the transition between regions 1 and 2 is larger for PVC–CPE than for PVC. Stress intensity factors in the interval 2.1–3.0 $MPa\,m^{1/2}$ resulted for the notched PVC–CPE specimens in air in a bending angle at the 1–2 transition of $(10 \pm 5) \times 10^{-3}$ rad. The larger angles correspond to the smaller stress intensity factors. In natural gas enriched with 60 000 p.p.m. benzene, the stress intensity factors applied to the PVC–CPE specimens were in the range 1.7–2.1 $MPa\,m^{1/2}$, and the corresponding bending angle was $(7 \pm 3) \times 10^{-3}$ rad. It is therefore concluded that the bending angle at the 1–2 transition is decreased a little by the presence of 60 000 p.p.m. benzene.

The bending angles at the 1–2 transition observed in the notched PVC specimens are lower than those observed in the PVC–CPE specimens, namely $(2 \pm 1) \times 10^{-3}$ rad. This interval holds for both the measurements in air and the measurements in natural gas enriched with 60 000 p.p.m. benzene. The applied stress levels were in the range 1.6–2.1 $MPa\,m^{1/2}$.

The actual bending rate is a function of the time to failure and of the craze renewal ahead of the crack tip. The bending rate will increase with a decreasing time to failure. The craze renewal will be a function of the stress intensity factor applied and of the critical craze fibril length. The higher bending rates in region 2 in natural gas enriched with 60 000 p.p.m. benzene compared to those observed in air suggests that the critical craze fibril length is increased by benzene vapour.

4.3. Fracture toughness versus temperature

In service, gaspipes will experience different temperatures. In general, the temperature will be in the interval from 5–10 °C. The temperature-dependent fracture toughness was studied over a broader temperature range in order to cover the extreme temperatures that sometimes occur.

The stress intensity factor as a function of the time to failure was obtained at -25, -10, 5 and 23 °C. The experimental data obtained are summarized in the stress intensity factor resulting in failure after 10^6 s versus temperature in Fig. 13. Notwithstanding the embrittlement found in impact tests on PVC and PVC–CPE gaspipes in the temperature range under study [21], the stress intensity factor leading to crack growth increases with decreasing temperature.

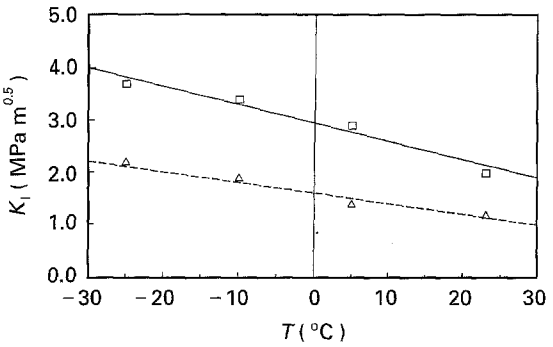

Figure 13 Stress intensity factor, K_I, corresponding to failure after 10^6 s as a function of the temperature, T, for (△) PVC and (□) PVC–CPE in air.

5. Discussion

The three-point bending experiments on PVC and PVC–CPE gaspipe materials in air, in natural gas enriched with 60 000 p.p.m. benzene, in low-pressure condensate, in high-pressure condensate, in *n*-octane and in 90%/10% *n*-octane/benzene, yield some interesting results: firstly, the lower fracture toughness of PVC–CPE in the environments studied compared to that found in air; secondly, the sometimes higher value of the fracture toughness of PVC in the environments studied compared to that found in air. Furthermore, the bending curves and the temperature-dependence of the fracture toughness are analysed in terms of critical craze dimensions.

5.1. Fracture toughness in air

Fracture toughness is quantified as the stress intensity factor corresponding to failure after a given loading period. For example, the time to failure is defined at 15 min by Holloway and Naaktgeboren [11]. In Table I, the results on the fracture toughness of PVC materials found in the literature are given. The variation in the K_I values presented in Table I is related to the PVC material (degree of gelation, molecular weight), the machining of the specimens, the heat treatment given to the specimen, the size of the specimen (plane strain/plane stress condition) and to the experimental conditions (loading and temperature). The values obtained in this study seem to be in the lower range of the values reported in the literature.

5.2. Fracture toughness in environments

K_I values for PVC materials obtained in gas environments are not available from the literature. The observed influence of benzene vapour, *n*-octane, an *n*-octane/benzene mixture and gas condensate on the fracture toughness of PVC and PVC–CPE has to be associated with sorption of vapour and liquid, because no chemical reactions occur between gas components and PVC. In a previous paper, it was shown that local sorption can result in plasticization and a reduction of the glass–rubber transition temperature [1]. However, the situation for a craze ahead of a crack is somewhat different from the situation of a surface craze. A surface craze is initiated after preferential sorption at a stress raiser. A craze ahead of a crack will be present directly after the load is applied. Therefore, sorption hardly affects the craze initiation ahead of a crack. On the other hand, the crack growth and the fracture toughness (see Equation 4) are related to the craze stability and thus are affected largely by sorption.

TABLE I Comparison of K_I values at crack initiation for PVC materials at ambient temperature

Reference	K_I (MPa m$^{1/2}$)	Specimen	Experiment
[11]	1.5–6.0	C-ring	Constant load
[6]	1.9–2.6	DEN tension	Constant strain rate
[10]	3.0	SEN bending	Constant strain rate
[22]	2.0–6.0	SEN tension	Constant strain rate
[7]	1.0–4.0	SEN bending	Constant load
This study	1.3–3.0	SEN bending	Constant load

TABLE II Experimental K_I values corresponding to failure after 10^6 s for PVC and PVC–CPE at 23 °C in some environments, together with the calculated volume fraction, v, liquid or vapour in the PVC matrix [1]

Environment	K_I (MPa m$^{1/2}$)		v (%)
	PVC–CPE	PVC	
Air	2.0	1.2	0
Benzene (30 000 p.p.m.)	1.1	1.3	5
Benzene (60 000 p.p.m.)	0.6	1.4	11
n-octane (l)	1.5	1.6	6
n-octane/benzene (90%/10%) (l)	1.0	1.2	12

In Table II, the stress intensity factor corresponding to failure after 10^6 s is presented, together with the calculated volume fraction of liquid or vapour in the PVC matrix. The volume fraction was calculated according to the procedure mentioned elsewhere [1]. For PVC, the stress intensity factor shows a maximum of 1.6 MPa m$^{1/2}$ at a volume fraction of 6%. Higher volume fractions of vapour or liquid in the PVC matrix give a decrease of the stress intensity factor concerned. For PVC–CPE, the situation is different. The concerned stress intensity factor is decreased by sorption in all environments studied. However, the magnitude of the decrease does not show a simple relationship with the calculated volume fraction in the PVC matrix. The benzene vapour (60 000 p.p.m.) seems to be more detrimental than the *n*-octane/benzene mixture (90%/10%). The reason for this phenomenon has to be related to the CPE phase.

5.3. Bending curves

The bending curves presented in Section 4.2 show that the presence of benzene vapour leads to an increase in craze dimensions. In slow crack growth experiments, in a first approximation, the craze dimensions will equal the static sizes, which can be calculated with Equations 1–3. The bending angle, θ, is related to the craze fibril length, δ_c, at the craze–crack transition by

$$\delta_c = \theta(W - a) \quad (7)$$

TABLE III Calculated δ_c value (Equation 8), experimental stress intensity factor, K_I, corresponding to failure after 10^6 s, calculated stress, σ_c, carried by craze fibrils (Equations 1 and 3) and calculated E modulus (Equation 4) for PVC and PVC–CPE in air and 60 000 p.p.m. benzene vapour at 23 °C

Material	Environment	δ_c (μm)	K_I (MPa m$^{1/2}$)	σ_c (MPa)	E (GPa)
PVC	Air	30	1.2	35	1.37
	Benzene (60 000 p.p.m.)	200	1.4	16	0.61
PVC–CPE	Air	125	2.0	29	1.10
	Benzene (60 000 p.p.m.)	150	0.6	8	0.30

where W represents the width of the specimen and a the crack length. For small bending angles, the bending angle is proportional to the magnitude of the bending, d (see Equation 4). Substitution of Equation 4 into Equation 7 then gives

$$\delta \approx \frac{d(W-a)}{40} \tag{8}$$

The value for $(W - a)$ /40 will decrease from 0.25 to a lower value due to crack growth. At the end of the interval with a constant bending rate (see Figs 9–12), the value of $(W - a)$ /40 is assumed to amount to 0.125. This value is substituted into Equation 8 together with the experimental value for d to calculate the craze fibril length, δ_c. The so-calculated values for δ_c are presented in Table III.

The craze length, a_c, can be obtained from the craze fibril length, δ_c, using Equation 3. Substitution of a_c and the experimental stress intensity factor corresponding to failure after 10^6 s yields the stress carried by the craze, σ_c. Afterwards, the modulus, E, can be obtained by substituting the experimental and calculated values into Equation 4. The calculated values for σ_c and E (see Table III) in air are in agreement with drawing stresses and moduli found experimentally. The low value of the stress intensity factor for PVC–CPE in benzene vapour (60 000 p.p.m.) is explained by the low stress-carrying capacity of the craze fibrils.

5.4. Temperature-dependence

The fracture toughness of PVC and PVC–CPE shows an increase with decreasing temperature. The data on the stress intensity factors presented in Fig. 13 can be evaluated using Equation 1. The stress, σ_c, can be associated with a drawing stress, σ_d. The macroscopic drawing stress was measured as a function of the loading time and the temperature. The values for the drawing stress corresponding to a loading time of 10^6 s, are presented in Table IV. Substitution of the values for the stress intensity factor and the drawing stress into Equation 1 then yields the craze length, a_c. The variation of the calculated a_c values is about 10% due to the limited accuracy of the experimental data on the stress intensity factors and the drawing stress.

It is remarkable that the craze length is not affected by the temperature in the temperature interval studied. For example, the brittle failure found for PVC in dumb-bell shaped specimens under a constant load at − 10 and − 25 °C does not result in a decrease of the craze dimensions.

TABLE IV Calculated a_c values (Equation 1) using the experimental stress intensity factor, K_I, and the experimental drawing stress, σ_d, corresponding to failure after 10^6 s for PVC and PVC–CPE at different temperatures

Material	Temperature (°C)	σ_d (MPa)	K_I (MPa m$^{1/2}$)	a_c (mm)
PVC	− 25	Brittle failure	2.2	–
	− 10	60	1.9	0.39
	5	50	1.4	0.30
	23	41	1.2	0.33
PVC–CPE	− 25	58	3.7	1.6
	− 10	50	3.4	1.8
	5	40	2.9	2.0
	23	32	2.0	1.5

6. Conclusion

The fracture toughness of PVC at 23 °C is hardly affected by the presence of benzene vapour, *n*-octane/benzene mixtures and gas condensate under conditions where the amount of aromatic components is limited (e.g. benzene content less than 60 000 p.p.m.). In some of the environments studied, a small increase in the fracture toughness was observed relative to the fracture toughness measured in air.

The fracture toughness of PVC–CPE at 23 °C is decreased by the presence of benzene vapour, *n*-octane/benzene mixtures and gas condensate. An enormous decrease, compared to the fracture toughness obtained in air at 23 °C, is observed in 60 000 p.p.m. benzene vapour.

The variations in the fracture toughness of PVC and PVC–CPE in the environments studied is explained by plasticization. Plasticization leads to an increase of the craze dimensions on the one hand, and to a decrease of the loading capacity of the craze on the other. The small variation in the fracture toughness observed for PVC suggests that the opposing phenomena are almost balanced. The decrease of the fracture toughness of PVC–CPE in the environments studied is explained by a domination of the decrease in load-carrying capacity of the craze fibrils.

The increase in fracture toughness of PVC and PVC–CPE with decreasing temperature, while the craze dimensions remain constant, indicates an increasing load-carrying capacity.

Acknowledgements

This work was sponsored by GASTEC, Nederlandse Gasunie and Ministerie van Economische Zaken. The author thanks Dr Ir. M. Wolters, Ir L. Oranje, Drs P. W. Peereboom, Professor Dr Ir J. van Turnhout and Dr K. E. D. Wapenaar, for valuable discussions, and Mr A. M. Ringenaldus and Mr C. H. B. van der Walle for performing the experiments.

References

1. J. BREEN, *J. Mater. Sci.* **28** (1993) 3769.
2. *Idem, ibid.* **29** (1994) 39.
3. X. LU and N. BROWN, *ibid.* **21** (1986) 2423.
4. *Idem, ibid.* **21** (1986) 4081.
5. A. LUSTIGER and R. D. CORNELIUSSEN, *ibid.* **22** (1987) 2470.
6. N. J. MILLS and N. WALKER, *Polymer* **17** (1976) 335.
7. G. P. MARSHALL, *Plast. Rubb. Proc. Appl.* **2** (1982) 169.
8. W. DÖLL and L. KÖNCZÖL, *Adv. Polym. Sci.* **91/92** (1990) 137.
9. W. DÖLL, *Polym. Eng. Sci.* **24** (1984) 798.
10. J. F. MANDELL, A. Y. DARWISH and J. F. McGARRY, *ibid.* **22** (1982) 826.
11. L. R. HOLLOWAY and A. J. NAAKTGEBOREN, *Plast. Rubb. Compos. Proc. Appl.* **15** (1991) 201.
12. J. G. WILLIAMS, G. P. MARSHALL, I. GRAHAM and E. L. ZICHY, *Pure Appl. Chem.* **39** (1974) 275.
13. J. G. WILLIAMS and G. P. MARSHALL, *Proc. R. Soc. Lond. A* **342** (1975) 55.
14. H. R. BROWN and T. H. CHIN, *J. Mater. Sci.* **15** (1980) 677.
15. E. J. KRAMER and E. W. HART, *Polymer* **25** (1984) 1667.
16. R. SCHIRRER, *Adv. Polym. Sci.* **91/92** (1990) 215.
17. S. J. ISRAEL, E. L. THOMAS and W. W. GERBERICH, *J. Mater. Sci.* **14** (1979) 2128.
18. R. A. W. FRASER and I. M. WARD, *Polymer* **19** (1978) 220.
19. J. L. S. WALES, Internal TNO report 268 (1981).
20. D. J. VAN DIJK, in "Proceedings of the Plastics Pipes VI", University of York, 26–28 March 1985, (PRI, London, 1985) p. 19.1.
21. T. G. MEIJERING, *Plast. Rubb. Proc. Appl.* **5** (1985) 165.
22. L. MASCIA, P. G. WOOLDRIDGE and M. J. STOKELL, *J. Mater. Sci.* **24** (1989) 2775.
23. E. J. KRAMER and L. L. BERGER, *Adv. Polym. Sci.* **91/92** (1990) 1.

Received 15 December 1993
and accepted 7 June 1995